

## **Chapter 2**

# **Analytic Method for Dynamic Analysis of the Track Structure**

With the ongoing operation of high-speed and heavy-haul railways, dynamic analysis of the track structure has become a significant research topic in the field of railway engineering. By establishing the continuous elastic beam model of track structure, analytic method for dynamic analysis of track structure is discussed, and characteristics of ground surface waves and the strong track vibration induced by high-speed trains are analyzed by the analytic method. Finally, effects of track stiffness on track critical velocity and track vibration are investigated.

### **2.1 Studies of Ground Surface Wave and Strong Track Vibration Induced by High-Speed Train**

It is understood that the increase in train speed may cause the increased dynamic action induced by the train on track and ground surface. This occurrence is especially serious under the high-speed operation. Studies have shown that when train speed reaches or exceeds some critical velocities, there would be surface waves induced by high-speed trains causing strong vibration of track structure. Meanwhile, owing to the wave propagation through ballast and subgrade, there would be strong vibration and structure-borne noise of surrounding buildings along the railway lines. In the track-ballast-subgrade-ground system, there are mainly two kinds of critical wave velocity: the wave velocity of Rayleigh wave on ground surface and the minimum phase velocity of the bending wave propagating in the track, which is also called track critical velocity. The track critical velocity varies according to different physical properties of the ground media. When the track foundation is soft subgrade, it is easy for high-speed trains to reach and exceed these two kinds of critical wave velocity. Madshus and Kaynia [1] from Sweden discovered this phenomenon in testing X2000 high-speed train. In the recent years, related studies have been emerging [1–5].

### 2.1.1 The Continuous Elastic Beam Model of Track Structure

To simplify the analysis, track critical velocity and strong track vibration are investigated by use of the analytic method in the following. The continuous elastic beam model of track structure is established as shown in Fig. 2.1.

According to D'Alembert principle, the differential equation for track vibration excluding damping is [6]

$$EI \frac{\partial^4 w}{\partial x^4} + m \frac{\partial^2 w}{\partial t^2} + kw = -F\delta(x - Vt) \quad (2.1)$$

where  $E, I$  stand for elasticity modulus and inertia moment around the horizontal axis;  $w$  is rail vertical deflection, and  $m$  is track mass per unit length;  $k$  is equivalent track stiffness, and  $\delta$  is Dirac function;  $V$  is train speed, and  $F$  is wheelset load.

Defining

$$\varepsilon_1^2 = \frac{m}{4EI}, \quad \varepsilon_2^4 = \frac{k}{4EI} \quad (2.2)$$

Equation (2.1) then can be transformed into

$$\frac{\partial^4 w}{\partial x^4} + 4\varepsilon_1^2 \frac{\partial^2 w}{\partial t^2} + 4\varepsilon_2^4 w = -\frac{F}{EI} \delta(x - Vt) \quad (2.3)$$

Firstly, let us consider the free vibration. Supposing  $F = 0$ , the solution for (2.3) is

$$w(x, t) = e^{\frac{i2\pi(x-ct)}{\lambda}} \quad (2.4)$$

where  $\lambda$  is vibration wavelength, and  $c$  is vibration wave propagation velocity.

Substituting (2.4) into (2.3), it has

$$c = \frac{1}{2\varepsilon_1} \left( \frac{\lambda^2 \varepsilon_2^4}{\pi^2} + \left( \frac{2\pi}{\lambda} \right)^2 \right)^{\frac{1}{2}} \quad (2.5)$$

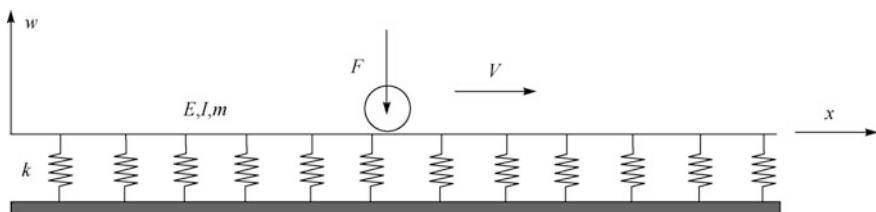


**Fig. 2.1** The continuous elastic beam model of track structure

When  $\lambda = \frac{\sqrt{2}\pi}{\varepsilon_2}$ ,  $c$  obtains the minimum, then there derives

$$c_{\min} = \sqrt[4]{\frac{4kEI}{m^2}} \quad (2.6)$$

$c_{\min}$  is the minimum phase velocity of the bending wave in track structure, also called track critical velocity.

Secondly, let us considering the wheelset load  $F$ , the solution is  $w(x - Vt)$ . Introducing  $z = x - Vt$ , Eq. (2.3) can be transformed into

$$\frac{\partial^4 w}{\partial z^4} + 4\varepsilon_1^2 V^2 \frac{\partial^2 w}{\partial z^2} + 4\varepsilon_2^4 w = -\frac{F}{EI} \delta(z) \quad (2.7)$$

Characteristic equation for (2.7) is

$$p^4 + 4\varepsilon_1^2 V^2 p^2 + 4\varepsilon_2^4 = 0 \quad (2.8)$$

The solution for the above characteristic equation is related to coefficient. When  $V < \frac{\varepsilon_2}{\varepsilon_1}$  (note: The existing domestic and international track structures all meet this inequality), the solution for (2.8) is

$$p = \pm\alpha \pm j\beta \quad (2.9)$$

where

$$\alpha = (\varepsilon_2^2 - V^2 \varepsilon_1^2)^{\frac{1}{2}}, \quad \beta = (\varepsilon_2^2 + V^2 \varepsilon_1^2)^{\frac{1}{2}} \quad (2.10)$$

Then, the solution for (2.7) should be

$$w(z) = e^{\alpha z} (D_1 \cos \beta z + D_2 \sin \beta z) + e^{-\alpha z} (D_3 \cos \beta z + D_4 \sin \beta z) + \varphi(z) \quad (2.11)$$

In the above equation,  $\varphi(z)$  is related to external load. When  $z = 0$ ,  $x$  is located at the wheel-rail contact point. When  $z \neq 0$  and  $\varphi(z) = 0$ , (2.11) can be turned into

$$\begin{aligned} w_1(z) &= e^{\alpha z} (D_1 \cos \beta z + D_2 \sin \beta z) & z \leq 0 \\ w_2(z) &= e^{-\alpha z} (D_3 \cos \beta z + D_4 \sin \beta z) & z > 0 \end{aligned} \quad (2.12)$$

Four undetermined coefficients in the above equations can be derived from four boundary conditions when  $z = 0$ . They are

$$w_1|_{z=0} = w_2|_{z=0}, \quad \left. \frac{\partial w_1}{\partial z} \right|_{z=0} = 0, \quad \left. \frac{\partial w_2}{\partial z} \right|_{z=0} = 0, \quad EI \left. \frac{\partial^3 w_1}{\partial z^3} \right|_{z=0} = \frac{F}{2} \quad (2.13)$$

The solution for (2.7) can be finally figured out as follows:

$$w(z) = -\frac{F}{8EI\alpha\epsilon_2^2} e^{-\alpha|z|} \left( \cos \beta z + \frac{\alpha}{\beta} \sin \beta|z| \right) \quad (2.14)$$

Under the multiple moving wheelset loads, the differential equation for track vibration is

$$EI \frac{\partial^4 w}{\partial x^4} + m \frac{\partial^2 w}{\partial t^2} + kw = - \sum_{i=1}^N F_i \delta(x - a_i - Vt) \quad (2.15)$$

where  $F_i$  is the load of the  $i$  th wheelset;  $a_i$  is the distance between the first wheelset and the  $i$ th wheelset;  $N$  is the total number of the wheelsets. The solution for (2.15) can be derived from the single moving wheelset solution (2.14) through superposition principle.

### 2.1.2 Track Equivalent Stiffness and Track Foundation Elasticity Modulus

The track equivalent stiffness  $k$  and the track foundation elasticity modulus  $E_s$  are closely related. Vesic [7] worked out the relationship between the track equivalent stiffness modeled as Euler beam on semi-infinite domain and the track foundation elasticity modulus. On such basis, Heelis [8] proposed the following formula for calculating track equivalent stiffness  $k$ .

$$k = \frac{0.65E_s}{1 - v_s^2} \sqrt[12]{\frac{E_s B^4}{EI}} \quad (2.16)$$

where  $E_s$  is the track foundation elasticity modulus (unit: MN/m<sup>2</sup>);  $v_s$  is Poisson's ratio;  $B$  is the sleeper length, usually 2.5–2.6 m;  $EI$  is the rail flexural modulus (unit: MN m<sup>2</sup>);  $k$  is the track equivalent stiffness (unit: MN/m<sup>2</sup>).

Under general circumstances, approximately the track foundation elasticity modulus  $E_s$  is 50 – 100 MN/m<sup>2</sup>. When  $E_s = 50$  MN/m<sup>2</sup> and Poisson's ratio  $v_s = 0.35$ , then  $k = 56.148$  MN/m<sup>2</sup> according to (2.16). In case of soft foundation,  $E_s = 10$  MN/m<sup>2</sup> or even lower, resulting in  $k = 9.82$  MN/m<sup>2</sup>.

### 2.1.3 Track Critical Velocity

As mentioned above, Eq. (2.6) is the computational formula for track critical velocity, which is related to the track equivalent stiffness  $k$ , the rail flexural modulus  $EI$ , and the track mass per unit length  $m$ . In calculating  $m$ , masses of the rail, sleeper, and ballast should be included. For instance, if the rail is 60 kg/m, with the sleeper allocation being 1760 sleepers/km, the ballast thickness 30 cm, the ballast shoulder breadth 35 cm, and the ballast density 2000 kg/m<sup>3</sup>, the track critical velocity corresponding to three different kinds of track foundation elasticity modulus can be calculated as shown in Table 2.1.

From Table 2.1, it can be observed that when  $E_s = 10 \text{ MN/m}^2$ ,  $c_{\min} = 91.34 \text{ m/s} = 328.8 \text{ km/h}$  and when  $E_s = 5 \text{ MN/m}^2$ ,  $c_{\min} = 75.70 \text{ m/s} = 272.5 \text{ km/h}$ . These two velocities can be easily exceeded by high-speed trains.

### 2.1.4 Analysis of Strong Track Vibration

#### 2.1.4.1 Analysis of Strong Track Vibration Under a Moving Wheelset Load

When the track foundation elasticity modulus  $E_s = 50 \text{ MN/m}^2$ , the track critical velocity  $c_{\min} = 141.24 \text{ m/s}$  according to Table 2.1. Supposing a wheelset load (axle load  $F = 170 \text{ kN}$ ) moving over the track at four different speeds, respectively ( $V = 110, 130, 135$ , and  $140 \text{ m/s}$ ), track vibration is analyzed accordingly, as is indicated by the track vibration deflection curve in Fig. 2.2. It can be seen from this figure that strong track vibration would be induced when the wheelset moves at the speed of  $140 \text{ m/s}$ , which is approaching the track critical velocity.

**Table 2.1** The track critical velocity corresponding to different track foundation elasticity modulus

Parameters	$E_s/(\text{MN/m}^2)$	$k/(\text{MN/m}^2)$	$EI/(\text{MN m}^2)$	$m/(\text{kg/m})$	$B/(m)$	$c_{\min}/(\text{m/s})$
Compacted clay	50	56.15	13.25	2735	2.5	141.24
Loam	10	9.82	13.25	2735	2.5	91.34
Soft subgrade	5	4.63	13.25	2735	2.5	75.70

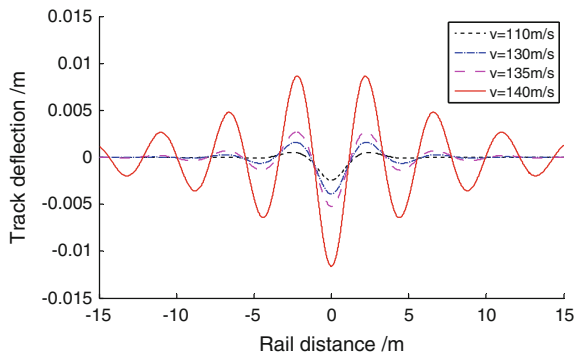


**Fig. 2.2** The track vibration deflections by a moving wheelset load at different speeds

#### 2.1.4.2 Analysis of Strong Track Vibration Induced by a High-Speed Train

Track vibration is investigated by Fig. 2.3, the computational model, when the high-speed train moves at different speeds. Supposing the train marshaled by one TGV high-speed motor car and four TGV high-speed trailers. Parameters for TGV high-speed motor car and trailers are given in Chap. 6. Computational results are presented in Figs. 2.4 and 2.5, which represent the track deflections for  $E_s = 50 \text{ MN/m}^2$  and  $E_s = 10 \text{ MN/m}^2$ , respectively. In these two figures, effects of two kinds of rail flexural stiffness  $EI$  on track deflection are shown, with the solid line being the track deflection for the flexural stiffness  $EI = 13.25 \text{ MN m}^2$  (namely the flexural stiffness for two rails of  $60 \text{ kg/m}$ ), and the dotted line being the track deflection for the flexural stiffness  $EI$  doubles (namely increasing two guard rails of  $60 \text{ kg/m}$ ).

Based on the above computational results, some conclusions are summarized as follows [9–11]:

- (1) When the train speed approaches the track critical velocity, strong track vibration will be induced, as is shown in Figs. 2.2, 2.4 and 2.5.
- (2) Track foundation elasticity modulus is the main factor for influencing the track critical velocity. In particular when the track foundation is the soft subgrade, the track critical velocity is much low, which can be easily exceeded by medium-speed or high-speed trains.

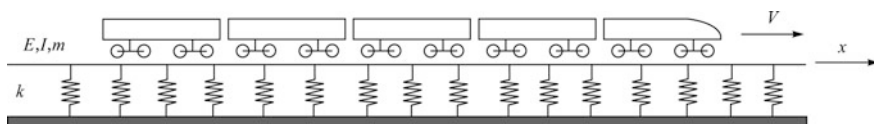


**Fig. 2.3** The computational model of a TGV high-speed train

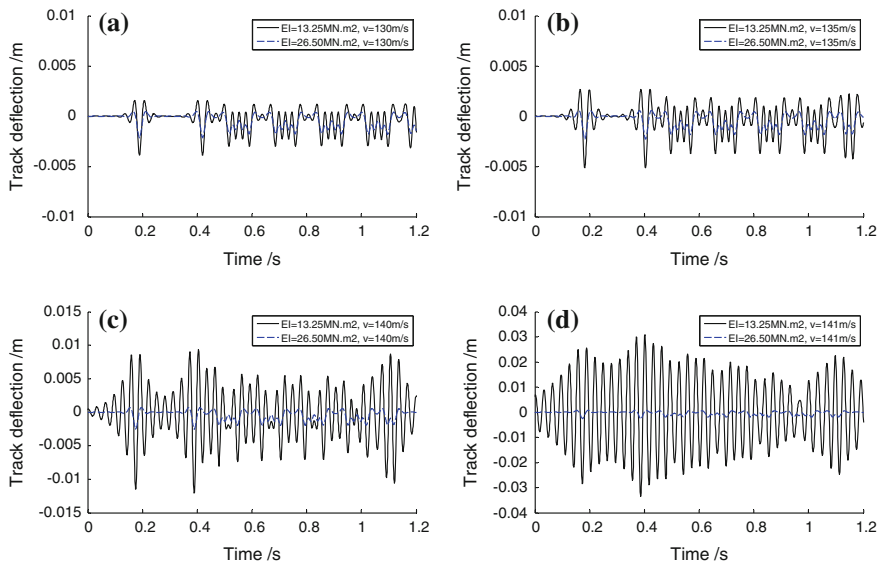


**Fig. 2.4** The track deflections for  $E_s = 50 \text{ MN/m}^2$ , **a** for train speed of 130 m/s, **b** for train speed of 135 m/s, **c** for train speed of 140 m/s and **d** for train speed of 141 m/s

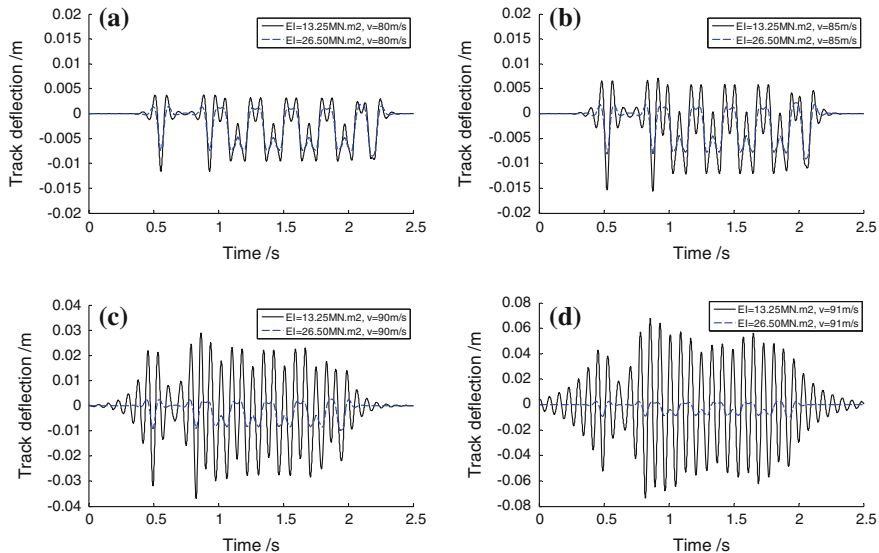


**Fig. 2.5** The track deflections for  $E_s = 10 \text{ MN/m}^2$ , **a** for train speed of 80 m/s, **b** for train speed of 85 m/s, **c** for train speed of 90 m/s and **d** for train speed of 91 m/s

- (3) When the train speed is lower than the track critical velocity, the increase in rail flexural stiffness has not obvious effects on reducing track deformation, as shown in Figs. 2.4a, b and 2.5a, b. However, when the train speed approaches the track critical velocity, the increase in the rail flexural stiffness has significant effects on track deformation reduction, as shown in Figs. 2.4c, d and 2.5c, d.
- (4) The rail flexural stiffness has certain effects on track vibration waveform and amplitude. When the rail flexural stiffness is small, the vibration waveform is multiple, and the amplitude is large and vice versa. When the train speed approaches the track critical velocity, this phenomenon is particularly obvious, as indicated in Figs. 2.4c, d and 2.5c, d. The more frequent the vibration is, the larger the amplitude is and the more likely it is for the ballast to come into liquefaction, which would reduce the stability of the track foundation.

## 2.2 Effects of Track Stiffness Abrupt Change on Track Vibration

In railway lines, there are a large number of bridges, grade crossings, and rigid culverts. In track transition from the subgrade to abutment, or grade crossing and/or culverts, there appears uneven track stiffness. In some cases, there would be track stiffness abrupt change. Experiments have shown that when the train moves through areas of stiffness abrupt change, additional dynamic action would be significantly induced resulting in large track deformation. The vehicle riding comfort would be damaged, or at worst, the train operation accident would be caused. There are abundant studies on uneven stiffness of railway track both at home and abroad [12–17], though with some findings, but are limited to experimental methods.

In this section, effects of track stiffness abrupt change on track vibration are investigated by the analytic method for dynamic analysis of track structure. By establishing the simplified analytic model, impacts of track irregularity, foundation stiffness, and train speed on track vibration are analyzed.

### 2.2.1 *Track Vibration Model in Consideration of Track Irregularity and Stiffness Abrupt Change Under Moving Loads*

To simplify the analysis, the analytic method is adopted to investigate the effects of track irregularity and stiffness abrupt change on track vibration under a moving wheelset load at constant speed  $V$ . The simplified analytic model is shown in Fig. 2.6. The coordinate origin is set at the point of stiffness abrupt change. On the left side of the origin, the track foundation stiffness is  $k_1$ , and the deflection is  $w_1$ ;



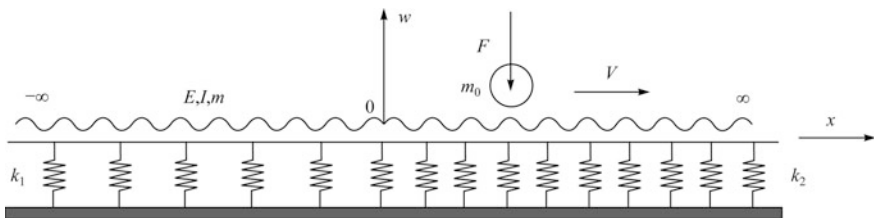


**Fig. 2.6** Track vibration model in consideration of track irregularity and stiffness abrupt change under moving loads

on the right side of the origin, the track foundation stiffness is  $k_2$ , and the deflection is  $w_2$ . Taking  $w_1$  for instance, according to D'Alembert's principle, the track vibration differential equation excluding damping is

$$EI \frac{\partial^4 w_1}{\partial x^4} + m \frac{\partial^2 w_1}{\partial t^2} + k_1 w_1 = - \left( F + m_0 \frac{\partial^2 (w_1 + \eta)}{\partial t^2} \right) \delta(x - Vt) \quad (2.17)$$

where  $E, I$  stand for track elasticity modulus and inertia moment around the horizontal axis;  $w$  is track vertical deflection;  $\eta$  is track irregularity;  $m$  is track mass per unit length;  $k_1$  is track foundation stiffness, and  $F$  represents the moving wheelset load;  $m_0$  is the wheelset mass;  $V$  is the wheelset moving speed, and  $\delta$  is Dirac function.

Supposing the track irregularity  $\eta$  is a cosine function

$$\eta = a \left[ 1 - \cos \frac{2\pi(x - Vt)}{l} \right] \quad (2.18)$$

In this function,  $a$  is the amplitude of track irregularity;  $l$  is the track irregularity wavelength.

Defining

$$\varepsilon_1^2 = \frac{m}{4EI}, \quad \gamma_1^4 = \frac{k_1}{4EI} \quad (2.19)$$

equation (2.17) can be transformed into

$$\frac{\partial^4 w_1}{\partial x^4} + 4\varepsilon_1^2 \frac{\partial^2 w_1}{\partial t^2} + 4\gamma_1^4 w_1 = - \frac{1}{EI} \left( F + m_0 \frac{\partial^2 (w_1 + \eta)}{\partial t^2} \right) \delta(x - Vt) \quad (2.20)$$

The solution for the above equation is related to  $(x - Vt)$ , in other words,  $w_1 = w_1(x - Vt)$ . By introducing  $z = x - Vt$ , (2.20) can be changed into

$$\frac{\partial^4 w_1}{\partial z^4} + 4\varepsilon_1^2 V^2 \frac{\partial^2 w_1}{\partial z^2} + 4\gamma_1^4 w_1 = -\frac{1}{EI} \left( F + m_0 \frac{\partial^2 (w_1 + \eta)}{\partial t^2} \right) \delta(z) \quad (2.21)$$

The characteristic equation for (2.21) is

$$p^4 + 4\varepsilon_1^2 V^2 p^2 + 4\gamma_1^4 = 0 \quad (2.22)$$

The solution for the above characteristic equation is related to coefficient. In case  $V < \frac{\gamma_1}{\varepsilon_1}$ , Eq. (2.22) can be solved into

$$p = \pm \alpha_1 \pm j\beta_1 \quad (2.23)$$

where

$$\alpha_1 = (\gamma_1^2 - V^2 \varepsilon_1^2)^{\frac{1}{2}}, \quad \beta_1 = (\gamma_1^2 + V^2 \varepsilon_1^2)^{\frac{1}{2}} \quad (2.24)$$

Thus, the solution for (2.21) can be obtained as

$$w_1(z) = e^{\alpha_1 z} (D_1 \cos \beta_1 z + D_2 \sin \beta_1 z) + e^{-\alpha_1 z} (D_3 \cos \beta_1 z + D_4 \sin \beta_1 z) + \varphi_1(z) \quad (2.25)$$

where  $\varphi_1(z)$  is related to external load. When  $z = 0$ ,  $x$  is located at the wheel-rail contact point. When  $z \neq 0$ ,  $\varphi_1(z) = 0$ ; when  $z \rightarrow -\infty$ ,  $w_1$  should be finite value; therefore,  $D_3 = D_4 = 0$ , and Eq. (2.25) can be transformed into

$$w_1(z) = e^{\alpha_1 z} (D_1 \cos \beta_1 z + D_2 \sin \beta_1 z) \quad z \leq 0 \quad (2.26)$$

where  $D_1, D_2$  are undetermined coefficients associated with the boundary conditions.

Similarly, the track vibration differential equation on the right side of the coordinate origin is

$$EI \frac{\partial^4 w_2}{\partial x^4} + m \frac{\partial^2 w_2}{\partial t^2} + k_2 w_2 = -\left( F + m_0 \frac{\partial^2 (w_2 + \eta)}{\partial t^2} \right) \delta(x - Vt) \quad (2.27)$$

where  $w_2$  is the vertical deflection of the right track, and  $k_2$  is the right track foundation stiffness. Following the solution method of (2.17), Eq. (2.27) can be solved to obtain

$$w_2(z) = e^{-\alpha_2 z} (D_3 \cos \beta_2 z + D_4 \sin \beta_2 z) \quad z \geq 0 \quad (2.28)$$

where

$$\alpha_2 = (\gamma_2^2 - V^2 \varepsilon_2^2)^{\frac{1}{2}}, \quad \beta_2 = (\gamma_2^2 + V^2 \varepsilon_2^2)^{\frac{1}{2}} \quad (2.29)$$

$$\varepsilon_2^2 = \frac{m}{4EI}, \quad \gamma_2^4 = \frac{k_2}{4EI} \quad (2.30)$$

$D_3, D_4$  are undetermined coefficients associated with the boundary conditions.

The four undetermined coefficients in (2.26) and (2.28) can be derived from the four boundary conditions when  $z = 0$ . They are

$$w_1|_{z=0} = w_2|_{z=0} \quad (2.31)$$

$$\left. \frac{\partial w_1}{\partial z} \right|_{z=0} = \left. \frac{\partial w_2}{\partial z} \right|_{z=0} \quad (2.32)$$

$$\left. \frac{\partial^2 w_1}{\partial z^2} \right|_{z=0} = \left. \frac{\partial^2 w_2}{\partial z^2} \right|_{z=0} \quad (2.33)$$

$$\left. -\frac{\partial^3 w_1}{\partial z^3} \right|_{z=0} + \left. \frac{\partial^3 w_2}{\partial z^3} \right|_{z=0} = - \left( \frac{F}{EI} + m_0 \frac{\partial^2 (w_2 + \eta)}{\partial t^2} \right) \Big|_{z=0} \quad (2.34)$$

Substituting (2.26) and (2.28) into the above four boundary conditions, the following solutions can be obtained through redundant derivation [17, 18].

$$w_1(z) = e^{\alpha_1 z} (C_1 \cos \beta_1 z + C_2 \sin \beta_1 z) C_3 \quad z < 0 \quad (2.35)$$

$$w_2(z) = e^{-\alpha_2 z} (C_1 \cos \beta_2 z + \sin \beta_2 z) C_3 \quad z \geq 0 \quad (2.36)$$

where

$$\begin{aligned} C_1 &= \frac{2\beta_2(\alpha_1 + \alpha_2)}{(\alpha_1 + \alpha_2)^2 + \beta_1^2 - \beta_2^2} \\ C_2 &= -\frac{\beta_2 \left[ (\alpha_1 + \alpha_2)^2 - \beta_1^2 + \beta_2^2 \right]}{\beta_1 \left[ (\alpha_1 + \alpha_2)^2 + \beta_1^2 - \beta_2^2 \right]} \\ C_3 &= -\frac{F + m_0 a \left( 2\pi V / l \right)^2}{EI(G_1 C_1 + G_2 C_2 + G_3 + G)} \\ G &= \frac{m_0 V^2}{EI} \left[ (\alpha_2^2 - \beta_2^2) C_1 - 2\alpha_2 \beta_2 \right] \end{aligned}$$

$$G_1 = -\alpha_1^3 - \alpha_2^3 + 3\alpha_1\beta_1^2 + 3\alpha_2\beta_2^2$$

$$G_2 = -3\alpha_1^2\beta_1 + \beta_1^3$$

$$G_3 = 3\alpha_2^2\beta_2 - \beta_2^3$$

From (2.35) and (2.36), the track accelerations can be derived as follows:

$$\frac{\partial^2 w_1}{\partial t^2} = V^2 e^{\alpha_1 z} \{ [(\alpha_1^2 - \beta_1^2)C_1 + 2\alpha_1\beta_1 C_2] \cos \beta_1 z + [(\alpha_1^2 - \beta_1^2)C_2 - 2\alpha_1\beta_1 C_1] \sin \beta_1 z \} C_3 \quad z < 0 \quad (2.37)$$

$$\frac{\partial^2 w_2}{\partial t^2} = V^2 e^{-\alpha_2 z} \{ [(\alpha_2^2 - \beta_2^2)C_1 - 2\alpha_2\beta_2 C_2] \cos \beta_2 z + [(\alpha_2^2 - \beta_2^2) + 2\alpha_2\beta_2 C_1] \sin \beta_2 z \} C_3 \quad z \geq 0 \quad (2.38)$$

Under multiple moving wheelset loads, the differential equation corresponding to (2.17) for track vibration is

$$EI \frac{\partial^4 w_1}{\partial x^4} + m \frac{\partial^2 w_1}{\partial t^2} + k_1 w_1 = - \sum_{i=1}^N \left( F_i - m_{0i} \frac{\partial^2 (w_1 + \eta)}{\partial t^2} \right) \delta(x - a_i - Vt) \quad (2.39)$$

where  $F_i$  is the moving load of the  $i$ th wheelset;  $m_{0i}$  is the mass of the  $i$ th wheelset;  $a_i$  is the distance between the first wheelset and the  $i$ th wheelset;  $N$  is the total number of the wheelsets.

The solution for (2.39) can be derived from the solution Eqs. (2.35) and (2.36) under a moving wheelset load through superposition principle.

### 2.2.1.1 Effects of Track Irregularity and Track Stiffness Abrupt Change on Track Vibration

It is verified that track vibration response is related to the track equivalent stiffness  $k_1, k_2$ , the rail flexural modulus  $EI$ , the track irregularity amplitude  $a$ , the wavelength  $l$ , the wheelset load  $F$ , the wheelset mass  $m_0$ , the wheelset moving speed  $V$ , and the track mass  $m$  per unit length. In calculating  $m$ , the mass of the rail, the sleeper, and the ballast should be included. In order to better probe into effects of track irregularity and track stiffness abrupt change on track vibration, the following analysis is conducted under two conditions of track regularity and irregularity (the periodic irregularity with wavelength  $l = 2$  m and amplitude  $a = 1$  mm) and in four cases of track stiffness ratio, namely  $k_2/k_1 = 1$ ,  $k_2/k_1 = 2$ ,  $k_2/k_1 = 5$ , and  $k_2/k_1 = 10$ . The track parameters under different conditions are as follows: the rail of 60 kg/m, the sleeper allocation of 1760 sleepers/km, the ballast thickness of

**Table 2.2** Computational parameters

Cases	$k_1/(\text{MN}/\text{m}^2)$	$k_2/(\text{MN}/\text{m}^2)$	$EI/(\text{MN}\cdot\text{m}^2)$	$m/(\text{kg}/\text{m})$	$m_0/(\text{kg})$	$F/(\text{KN})$
Case 1	$k_2$	118	13.25	2735	2000	170
Case 2	$\frac{k_2}{2}$	118	13.25	2735	2000	170
Case 3	$\frac{k_2}{5}$	118	13.25	2735	2000	170
Case 4	$\frac{k_2}{10}$	118	13.25	2735	2000	170

30 cm, the ballast shoulder breadth of 35 cm, the ballast density of  $2000\text{ kg}/\text{m}^3$ , and the track foundation elasticity modulus  $E_s = 100\text{ MN}/\text{m}^2$ , as is clearly shown in Table 2.2.

2.2.1.2 Analysis of Track Vibration Under a Moving Wheelset Load

Track vibration is analyzed under a moving wheelset load at different speeds  $V = 60, 70, 80$ , and  $90\text{ m/s}$ . Meanwhile, four kinds of track stiffness abrupt change and two conditions of track regularity and irregularity (the wavelength  $l = 2\text{ m}$  and amplitude  $a = 1\text{ mm}$ ) are taken into account as well. Relationships between the track deflection and the total amplitude of acceleration with the wheelset moving speed are indicated in Figs. 2.7 and 2.8. The total amplitude of acceleration is defined as the difference between the maximum and the minimum of the vibratory magnitude.

2.2.1.3 Analysis of Track Vibration Induced by a High-Speed Train

Analysis of track vibration is carried out for a high-speed train passing at the speed  $V = 90\text{ m/s}$ . The train is marshaled by one TGV high-speed motor car and four

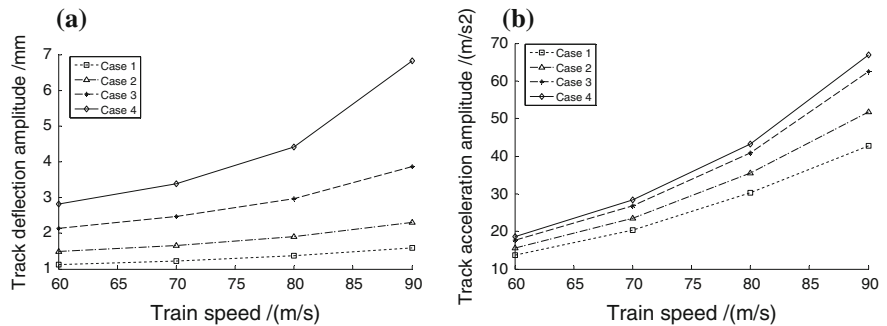


**Fig. 2.7** The track deflection amplitude and the track acceleration amplitude for smooth track under a moving wheelset load: **a** The track deflection amplitude and **b** the track acceleration amplitude

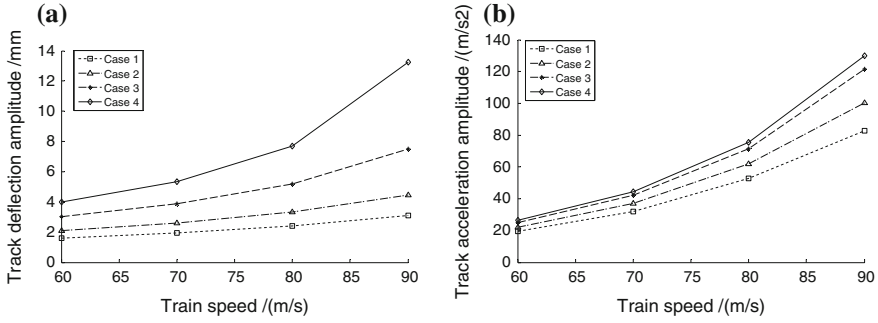


**Fig. 2.8** The track deflection amplitude and the track acceleration amplitude for track irregularities ( $a = 1$  mm) under a moving wheelset load: **a** the track deflection amplitude and **b** the track acceleration amplitude

TGV high-speed trailers (computational parameters for TGV high-speed motor car and trailers are noted in Chap. 6). The computational model is shown in Fig. 2.9. Four kinds of track stiffness abrupt change and two conditions of track regularity and irregularity (the wavelength  $l = 2$  m and amplitude  $a = 1$  mm) are taken into account for analyzing the track vibration. Computational results include the track deflection, velocity, acceleration, and time history curve of wheel-rail force at the point of stiffness abrupt change, as can be seen in Figs. 2.10, 2.11, 2.12 and 2.13. Figure 2.14 shows the dynamic coefficient curve for smooth track with different track stiffness ratio.

From the above computational results, conclusions can be drawn as follows [17, 18]:

- (1) Track stiffness abrupt change has effects on track vibration. As is shown in Figs. 2.7, 2.8, 2.10 and 2.13, the bigger the difference of track stiffness ratio is, the larger the dynamic response is induced.
- (2) For the fixed track stiffness ratio, the faster the train speed is, the larger the dynamic response of the structure is induced. This is clearly presented in Figs. 2.7 and 2.8.

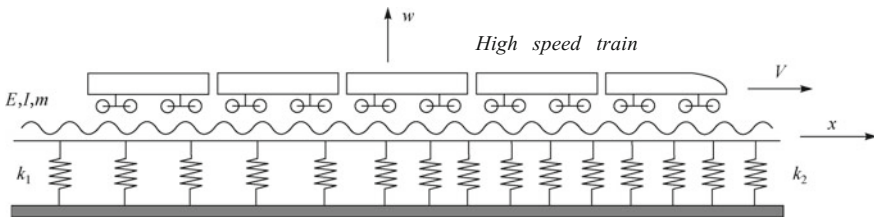


**Fig. 2.9** Analysis model of the track vibration induced by a high-speed train

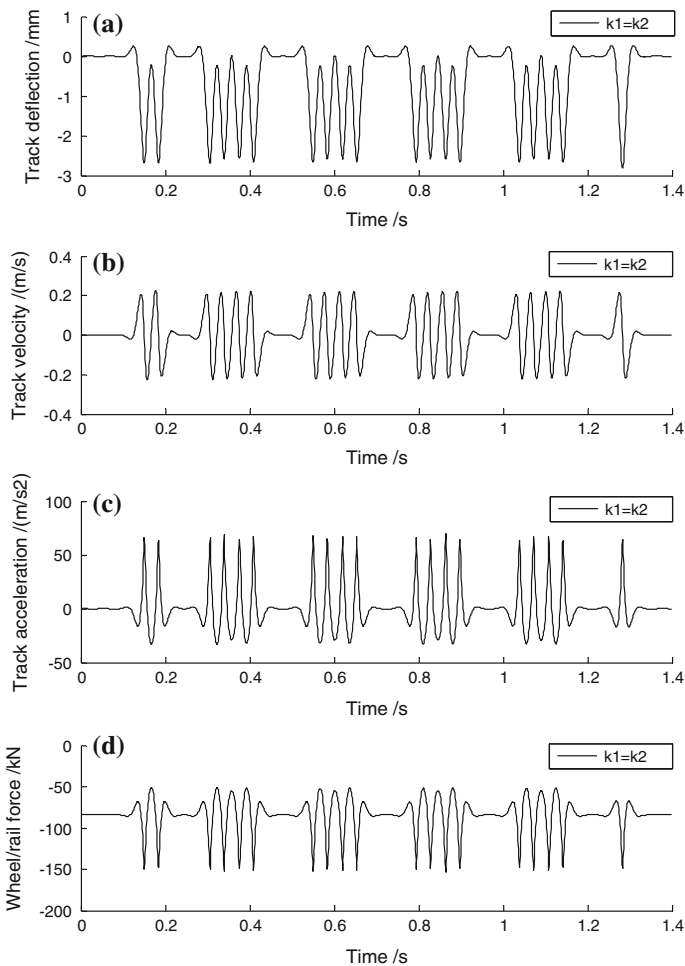


**Fig. 2.10** Time history of the track deflection, velocity, and acceleration as well as the wheel-rail force at the point of stiffness abrupt change ( $k_1 = k_2$ ,  $a = 1$  mm)

- (3) Track irregularity has significant impact on track vibration. The bigger the track irregularity amplitude is, the larger the dynamic response of the structure is induced.
- (4) When track stiffness ratio  $k_2/k_1 = 2$ ,  $k_2/k_1 = 5$ , and  $k_2/k_1 = 10$ , the total amplitude of the track deflection is 1.44, 2.42, and 4.27 times of those of the uniform track stiffness, and the total amplitude of the track velocity is 1.27, 1.84, and 2.73 times of those of the uniform track stiffness. In addition, the total amplitude of the track acceleration and the wheel-rail force is 1.18, 1.38, and 1.43 times of those of the uniform track stiffness. As for the acceleration and the wheel-rail force, the two parameters, which exert rather bigger influence on track structure, have greater effects on track vibration if the track

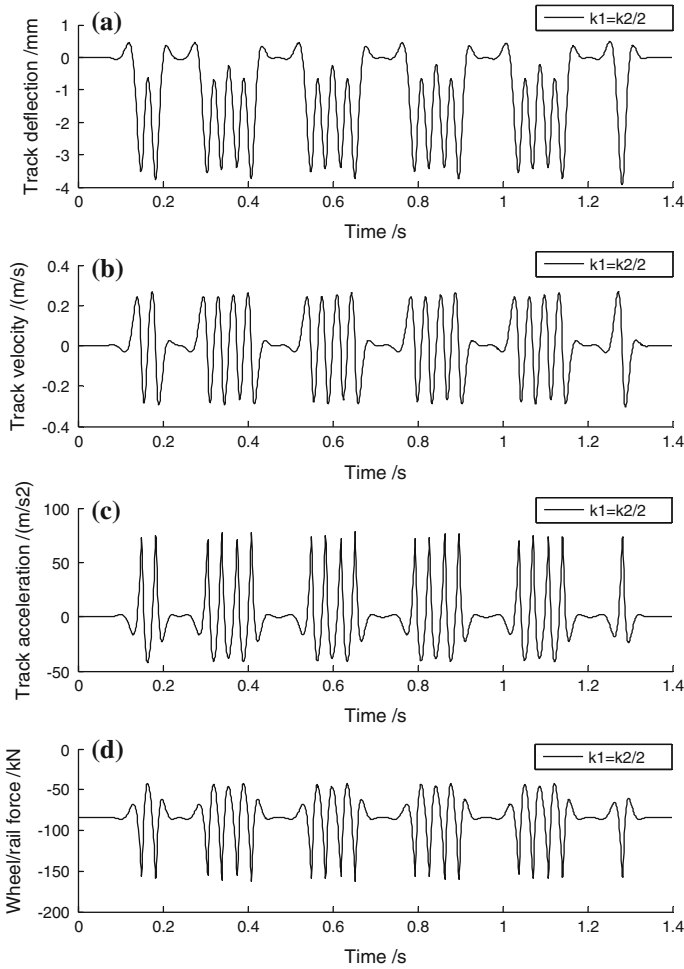


**Fig. 2.11** Time history of the track deflection, velocity, and acceleration as well as the wheel-rail force at the point of stiffness abrupt change ( $k_1 = \frac{k_2}{2}$ ,  $a = 1$  mm)

stiffness difference is within the range of 5 times; their effects on track vibration are on the decrease if the track stiffness difference is over 5 times. These are illustrated in Figs. 2.7 and 2.8.

- (5) The total amplitude represents the amplitude of structural vibration. The enlarged amplitude signifies the stronger structural vibration, which may cause subgrade liquefaction and reduce the stability of the structural foundation. When the track stiffness ratio reaches five times or more, the upper and lower oscillation waveform amplitude is approximate, which is harmful to track structural stability and should be avoided. These are illustrated in Figs. 2.12 and 2.13.



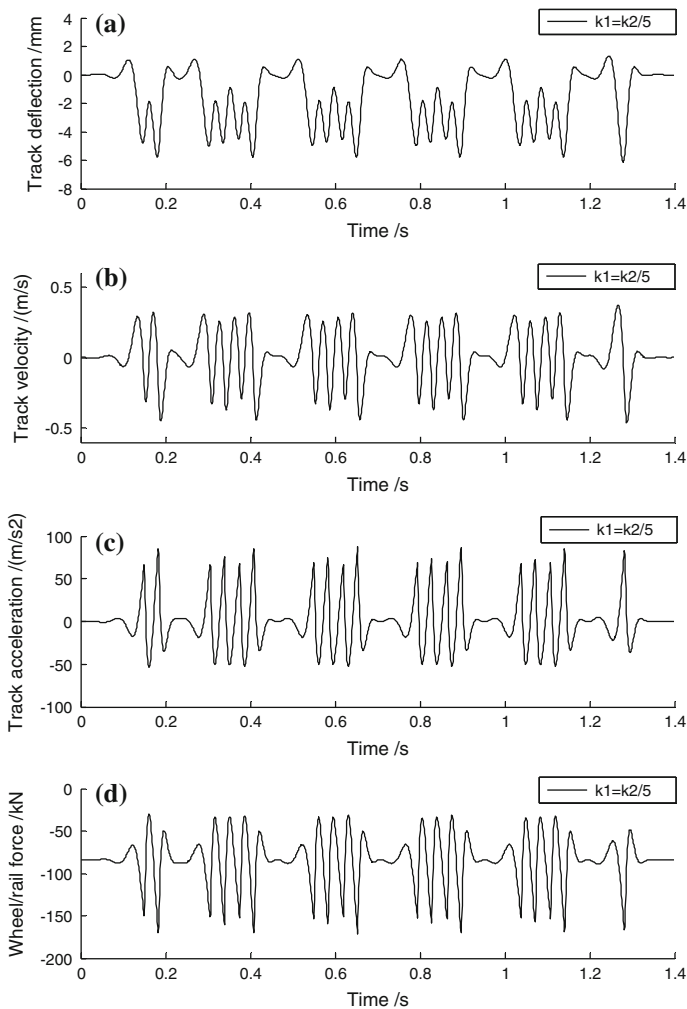


**Fig. 2.12** Time history of the track deflection, velocity, and acceleration as well as the wheel-rail force at the point of stiffness abrupt change ( $k_1 = k_2/5$ ,  $a = 1$  mm)

### 2.2.2 The Reasonable Distribution of the Track Stiffness in Transition

The reasonable distribution of the track stiffness in transition should meet the following requirements:

- (1) Ensure the equal track stiffness in track transition as much as possible.
- (2) Make sure smooth transition of track stiffness if it is hard to guarantee the equal stiffness so that track dynamic deflection, acceleration, and wheel-rail

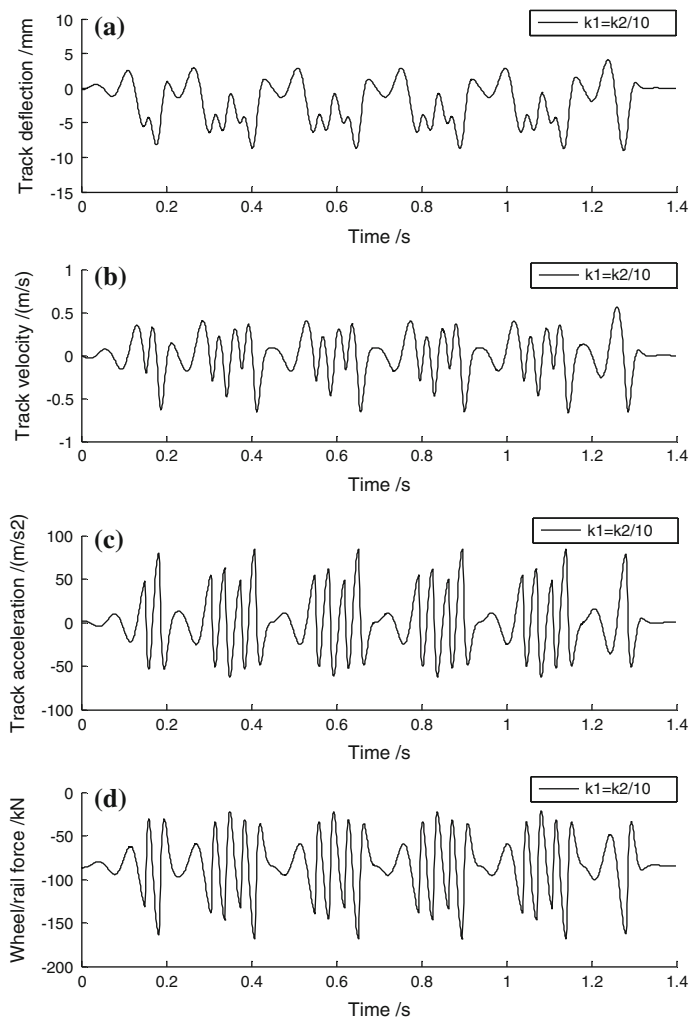


**Fig. 2.13** Time history of the track deflection, velocity, and acceleration as well as the wheel-rail force at the point of stiffness abrupt change ( $k_1 = \frac{k_2}{10}$ ,  $a = 1$  mm)

contact force would not change too much, thus resulting in great impacts to track transition.

For smoothing track stiffness in transition, it is advisable to install elastic rail pad on sleepers at rigid zones or lay rubber layer or ballast under the sleepers in order to increase the elasticity of the related section. It is also feasible to increase the track foundation stiffness by use of long sleepers, guard rails at transition sections, and the concrete approach slab and bolster at bridgehead. Besides, for increasing the

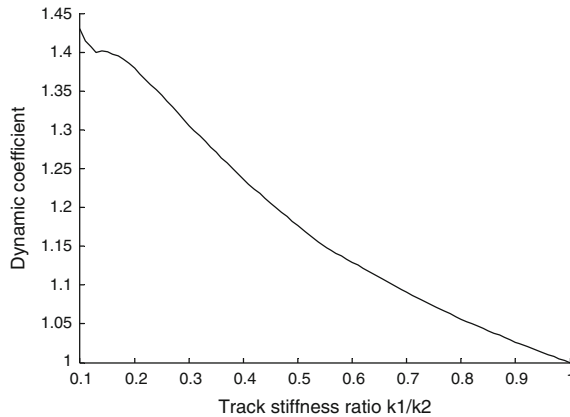


**Fig. 2.14** The dynamic coefficient curve for smooth track with different track stiffness ratio

track stiffness, it is preferable to lay geosynthetic material on the ballast bottom, replace the sand layer with asphalt mortar, or adopt coarse ingredients filling and reinforced soil embankment. The distance for smooth transition of track stiffness depends on the train speed, which shows the faster the speed is, the longer the distance is [19].

According to results of Fig. 2.14, when  $k_1/k_2 \geq 1/2$ , the dynamic coefficient  $\alpha = 1.17$ . Based on this, the following suggestions are proposed for the design of the reasonable track stiffness in transition: (1) adopting the stratified reinforcement at the transition sections, usually 3–4 layers, for convenient construction. (2) The dynamic coefficient induced by train in track transition and the stiffness ratio of each layer should meet such conditions as  $\alpha \leq 1.2$  and  $1/2 \leq k_1/k_2 \leq 1$ . (3) The distance of smooth transition for each layer is  $l = 5 - 10$  m. When the train speed  $V \leq 160$  km/h, then  $l = 5$  m, and when the train speed  $V > 160$  km/h, then  $l = 10$  m. This is illustrated in Fig. 2.15.

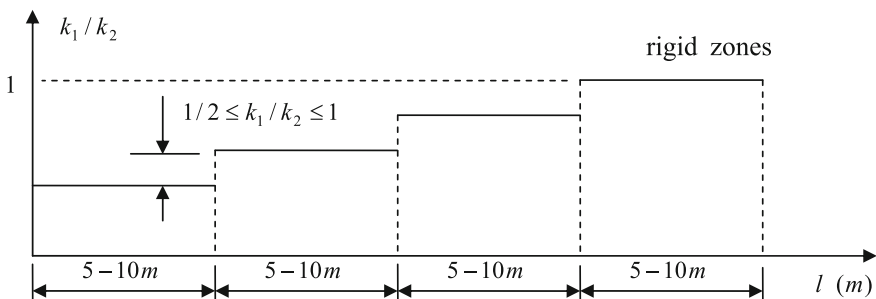


**Fig. 2.15** Track stiffness at the stratified reinforcement transition section

## References

1. Madshus C, Kaynia A (1998) High speed railway lines on soft ground: dynamic response of rail-embankment-soil system. NGI515177-1
2. Krylov VV (1994) On the theory of railway induced ground vibrations. *J Phys* 4(5):769–772
3. Krylov VV (1995) Generation of ground vibrations by super fast trains. *Appl Acoust* 44:149–164
4. Krylov VV, Dawson AR (2000) Rail movement and ground waves caused by high speed trains approaching track-soil critical velocities. *Proc Instit Mech Eng Part F J Rail Rapid Transit* 214 (F):107–116
5. Xiaoyan Lei, Xiaozhen Sheng (2004) *Railway traffic noise and vibration*. Science Press, Beijing
6. Belzer AI (1988) *Acoustics of solids*. Springer, Berlin
7. Vesic AS (1961) Beams on elastic subgrade and the Winkler hypothesis. In: *Proceedings of the 5th international conference on soil mechanics and foundation engineering vol 1*. Paris, France, pp 845–851
8. Heelis ME, Collop AC, Dawson AR, Chapman DN (1999) Transient effects of high speed trains crossing soft soil. In: Barends et al. (eds) *Geotechnical engineering for transportation infrastructure*. Balkema, Rotterdam, pp 1809–1814
9. Lei X, Sheng X (2008) *Advanced studies in modern track theory*, 2nd edn. China Railway Publishing House, Beijing
10. Lei X (2006) Study on critical velocity and vibration boom of track. *Chin J Geotech Eng* 28 (3):419–422
11. Lei X (2006) Study on ground waves and track vibration boom induced by high speed trains. *J China Railway Soc* 28(3):78–82
12. Kerr AD, Moroney BE (1995) Track transition problems and remedies. *Bull 742-Am Railway Eng Assoc Bull* 742:267–297
13. Kerr AD (1987) A method for determining the track modulus using a locomotive or car on multi-axle trucks. *Proc Am Railway Eng Assoc* 84(2):270–286
14. Kerr AD (1989) On the vertical modulus in the standard railway track analyses. *Rail Int* 235 (2):37–45
15. Moroney BE (1991) A study of railroad track transition points and problems. Master's thesis of University of Delaware, Newark
16. Lei X, Mao L (2004) Dynamic response analyses of vehicle and track coupled system on track transition of conventional high speed railway. *J Sound Vib* 271(3):1133–1146
17. Lei X (2006) Effects of abrupt changes in track foundation stiffness on track vibration under moving loads. *J Vibr Eng* 19(2):195–199
18. Lei X (2006) Influences of track transition on track vibration due to the abrupt change of track rigidity. *China Railway Sci* 27(5):42–45
19. Liu L, Lei X, Liu X Designing and dynamic performance evaluation of roadbed-bridge transition on existing railways. *Railway Stand Des* 504(1):9–10

<http://www.springer.com/978-981-10-2037-7>

High Speed Railway Track Dynamics  
Models, Algorithms and Applications

Lei, X.

2017, XXII, 414 p. 269 illus. in color., Hardcover

ISBN: 978-981-10-2037-7